SIMULATION OF THE COOLING EFFECT OF THE ROOF ADDED PHOTOVOLTAICS

Vasilis C Kapsalis[*1], Eftychios Vardoulakis and Dimitris Karamanis[*1]

1 Department of Environmental & Natural Resources Management, University of Patras
Seferi 2, 30100
Greece
**Corresponding authors: bkapsal@central.ntua.gr, dkaraman@cc.uoi.gr*

ABSTRACT

In this study, the TRNSYS simulation engine was used to investigate the shading and cooling effect of roof added photovoltaics. The local weather conditions were introduced in the data reader component. The sol air effective temperatures were modeled in the roof –air boundary layer, while a single zone model was used for the heat transfer calculation, both in bared and PV shaded roof. The simulation was validated by experimental data of a PV installation at the roof of the Department of Environmental & Natural Resources Management. The simulation results show that photovoltaic panels have a high impact on the roof surface temperature between shaded and exposed parts of the roof during the summer time. Heat transfer simulation with or without roof integrated photovoltaic shadings revealed the factors influencing cooling loads of a building during the year. The roof added photovoltaics can passively reduce the daily rooftop cooling energy and peak load during the hot summer days in addition to electricity production.

KEYWORDS

Roof added photovoltaics, temperature effect, heat flux, cooling load, peak power demand

1 INTRODUCTION

In countries with elevated temperatures during summer, like Greece, heat is the main problem of human thermal discomfort in buildings. The problem has intensively increased during the last 30 years since the lack of any urbanization plan led to uncontrollable growing with the subsequent environmental impact like the heat island effect in the major cities (Santamouris M. et al, 2001, Giannopoulou K. et al, 2010). The effect is lately observed regardless of the city size (Vardoulakis E. et al, 2011). Air conditioning is primary the only technique to compensate the increased temperatures and contributes a significant percentage of the total energy consumption of buildings in Greece. Subsequently, almost 25% more electricity is needed for a very short summertime period, especially July and August, and is mainly produced from fossil fuels. Many alternatives solutions have been proposed with some of them being partially effective with specific applications today (Vardoulakis E. et al., 2011, Karamanis D. et al., 2012, Synnefa A. et al, 2006, Alvarado J.L. et al, 2009). In the proposed solutions, the primary objective is the reduction of the buildings cooling load and the blocking of the temperature rise inside the urban spar during the summertime.

In addition, much research has been conducted on the direct use of rooftop building added PV (BAPV) for energy production (Strzalka A. et al, 2012, James P.A.B at al, 2009). In contrast, the possible indirect benefits of PV installations in buildings have been mainly concentrated in their integration on the building envelope and façade and their use as shading devices, blinds, walls, tiled roofs and windows. However, rooftop PV systems such as building

shading of the uncovered surface have received much less attention, while the Pv installed capacity in buildings roofs have been increased, almost linearly, approaching the 180 MW at the end of June 2012 (Greek operator of electricity market, 2012). While a number of simulation studies have been conducted, systematic experimental measurements are limited with the exception of a recent experimental study on the roof temperature variation for a limited time period (Dominguez A. et al, 2011). For example, it was demonstrated by heat transfer simulation into four different types of roofs, that BAPV can change the thermal resistance of a building by adding or replacing the building elements (Wang Y. 2006, Tian W. et al 2009). For ventilated air gap BAPV, decreases of 46% and 51% occurred for the daily heat-gain and the peak-cooling load compared with the conventional roof. Simulation results also showed that building surface temperature significantly changes while urban canyon air temperature alters only marginally. Also, Yang et al. (Yang et al, 2001) developed a simulation model for the thermal performance of PV roofs and found that the cooling load component through a PV roof is about 35% of the load of a conventional roof. In the recent experimental study, air temperature sensors and data measurements were collected for the period from 12 to 20 of August 2012. Simulations showed a reduction to the cooling load and peak power demand for the specified period. However, recent comparative simulated impact studies of roof installations, provided evidence that white and green roofs are more effective strategies for urban heat island mitigation than their PV covered ones (Scherba A. et al, 2011). In view of the above, the objective of the present study was to systematically investigate the temperature and heat gain variation of a rooftop PV installation on a university building during the summer and gain a better insight in the shading mechanism of roof added photovoltaics. PV and roof temperatures as well as meteorological parameters were recorded to estimate the differences into roof heating for shaded and non-shaded roof while the cooling and heating loads throughout the year were determined by extensive heat transfer simulation.

2 PV AND ROOF TEMPERATURES

2.1 Experimental Data

Measurements were conducted in the city of Agrinio (Western Greece) during August 2012 on a building roof of the University. Hobo dataloggers (model: Hobo ProV2) and thermocouples (Omega TMQSS-OM075G-300) connected with a fully automated meteorological station were used to collect the temperature data. The configuration and exact positions of the temperature sensors are depicted in Fig. 1.

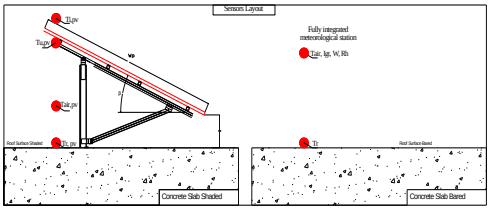

Figure 1: Sensors layout

In Figure 2.1a, temperature variations for roof surface with PV shading (Tr,pvm) and exposed roof (Tr m) are presented for the studied period from 12 to 20 August 2012. During the daytime, the temperature difference between shaded and exposed roof reached a maximum at 1:00 pm every day. At this time, maximum difference reached 16.2 ^{o}C on the first day of the measurements (12 August 2012) and a minimum difference of 10.7 ^{o}C on the ninth day of the

measurements (16 August 2012). The opposite effect was taking place after the sunset till sunrise. Exposed roof reached lower temperature levels compared to shaded roof. This difference was explained by the increased long wave radiation loss of the exposed roof surface and much more effective cooling during the night, compared to the part of the roof lying under the PV. The reason of the better and faster cooling is the increased sky view factor of the exposed roof, in addition to the shaded roof, proving that PV has also insulating properties. This result is in agreement with similar observations (Dominguez A. et al, 2011).

The variability of the roof surface temperature was also daily monitored. On a typical summer day, exposed roof summer temperature started from the value of 16.5 ^{o}C (at 6:00 am) and reached a maximum of almost 55 ^{o}C at noon. In contrast, shaded roof temperature started to rise at 20.3 ^{o}C (at 6:00) and reached a peak at 38.6 ^{o}C (at 1:00 pm). This indicates higher rates of heat absorption from exposed roof that could potentially lead to higher degradation of the roof construction materials and buildings insulation.

Figure 2.1b shows the temperatures over and under the PV module surface and air temperature between the PV tilted array and the shaded roof surface. PV surface temperature (Ti,pv) is almost 13 ^{o}C to 15 ^{o}C hotter compared to the temperature exactly under the PV module (Tu,pv) at the time period of the maximum solar radiation. This finding indicates that BAPV can act as an extra insulation over the roof during the summertime, absorbing a large amount of heat while simultaneously producing electricity.

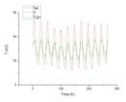

Figure 2.1a: Temperature variation for exposed and PV shaded roof

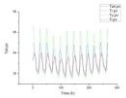

Figure 2.1b: Temperatures over and under PV

2.2 TRNSYS Simulation

Following the temperature measurements, a heat transfer simulation analysis was performed in order to examine the influence of BAPV in the building's cooling loads during the specified period. The calculation method of the program is based on the TRNSYS simulation engine (TRNSYS user manual, (2010). The local meteorological parameters were used and introduced in the program. The modelled components of the engine machine were built up through a step by step procedure. The calibration was based on several outputs of independent stages, respectively. The solar irradiation distribution produced by the TRNSYS is similar to that attained from the nearest local TMY data (Figure 2.2a). The PV array operation temperature and power at MPP are in accordance with those expected by the verified properties at STC conditions (Figure 2.2b). The single zone building utilizes the specified heat loss coefficient as of the materials properties and the capacitance is a lumped value derived from the sum of the specific heat capacities of the building's envelope. Finally the study of the roof module with and without PV panel simulated the heat transfer process with the utilization of the effective conductance and sol air temperature.

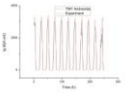

Figure 2.2a: Experiment radiation and TMY nearest local data

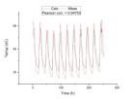

Figure 2.2b: PV array temperature at MPP power

Temperatures were modeled according to the following assumptions:

i. the body is gray
ii. the radiation properties are independent of the wavelength and
iii. the body is non transparent

According to built in components of the simulation engine, an extended analysis was performed to simulate the features of the building's response to the phenomenon. The weather conditions of a local meteorological station and the Hobo data loggers, such as total radiation Ig, wind velocity W and air temperature Tair, were collected and introduced into the data reader component. The same air velocity was used in both cases, with and without PVs, in order to express the dependence of the forced convection coefficient ho on it, as

$$ho = 5.7 + 3.8W, \quad (2)$$

in (Kj/h/m^2.^{o}C) with W, the wind velocity (m/s).
The temperature of surrounding medium was initially expressed with the solair temperature for the exposed roof surface and modeled, as the result of energy balance of total radiation and forced convection of roof – air boundary layers. The *e* correction factor was used to explain the heat flux between the internal and external roof and humidity. In our model this factor as a function of total radiation and the external convection coefficient ho, is chosen so that:

$$\lim_{Ig\to 0} e = ho \quad (3)$$

$$Tsa = Tair + \alpha Ig/ho - \varepsilon \Delta R/ho \mp e \quad (4)$$

where Tsa is the sol air temperature (^{o}C), Tair, the air temperature (^{o}C), α the absorptivity, ($0<\alpha<1$), ε the emissivity coefficient ($0<\varepsilon<1$) Ig the total horizontal radiation ($\frac{KJ}{hm^2}$), ΔR the diffuse radiation and sky temperature effect ($\frac{KJ}{hm^2}$).
The absorption coefficient best fit value calibration was found to be α = 0.45 which is between flair flagstone's and gravel's material and denotes an albedo value for the area within the typical range of the climate conditions at the specified period (e.g dew point and participated water). The emissivity value was selected as ε=0.80. Measured and calculated data for the exposed roof sol – air temperature were validated and the results are presented in Figure 3a.
At the same time, the sol – air effective temperature of the PV shading roof, was derived from a more complicated process. The PV cell acts as an absorber with a (τα) coefficient, and its operating temperature depends on Normal Operation Cell Temperature (NOCT) conditions, the total radiation Ig and the air temperature Tair. The temperature below the array is a combined calculation between the heat transfer through the panel with a heat transfer coefficient U_L and the air convection between the cell operating temperature and the air temperature. The effective emissivity (ASHRAE, 2013) coefficient was used in this case to express the influence of the two bodies temperatures, the surface and the back edge of the array, and is deduced as.

$$\varepsilon eff = \frac{1}{\frac{1}{\varepsilon e}+\frac{1}{\varepsilon c}-1}, \quad (5)$$

where εe, the emitter's emittance with a value of 0.5 for the white plastic membrane, and εc, the collector's emittance, with a value of 0.80 for the surface material as above.
According to the observed data, during the day, the PV back temperature is higher than the one on the surface under the PV, while in the late afternoon (19:00 or 20:00) the reverse process begins and the surface temperature is slightly higher, about 1 to 3 ^{o}C, until the first sunset time.
Thus, the shaded roof absorbs the diffused only radiation and a small portion of the total, depending on the sky view factor, while the Boltzman emissivity depends on a different temperature than the sky's one, because, as denoted, it faces the PV back surface. Then the longwave emission term (LW) comes from the infrared radiation difference between the roof and the PV back edge. In this case, the total horizontal radiation has to be decomposed in $It =$ Ib + Id, which was done by the radiation processor using the Reindl model, since the roof is horizontal and the factors Fgnd = 0 and Fsky = 1. The roof fraction factor was assumed to be 0 and that only the diffused radiation affects the PV shaded roof. Roof surface was considered to be 0.81 cm^2 (0.9 cm x 0.9 cm), with one PV panel on it. The exposed roof model was extended with the available TRNSYS components and the necessary modifications to match the PV shaded roof conditions as prescribed were implemented. Also, the temperature distribution, the air gap effect and the heat flux downwards or upwards the internal roof surface have been taken into account. The effective sol air temperature and the heat rate were calculated with the TRNSYS simulation. In figure 2.2c, 2.2d the measured and calculated temperature values are presented.

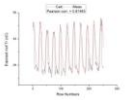

Figure 2.2c: Exposed roof surface temperature

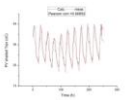

Figure 2.2d: PV shaded roof surface temperature

2.3 HEAT FLUXES IMPACT OF THE ROOF INTEGRATED PHOTOVOLTAICS ON THE BUILDING'S THERMAL BEHAVIOR

A single floor residence building of rectangular shape and 81 cm^2 flat roof was adopted for the simulation. For simulating the PV shading, a PV panel were installed on the flat roof at a tilt angle of 30 °. The lumped capacitance method was used to define the zone temperature of the building and as an input for the heat transfer simulation of the roof to the ceiling or backwards. The building's energy demand response was simulated for the specified period before and after installing the PV.
Initially, the effect of the structural materials on cooling loads was studied. Two insulation scenarios are simulated with two building thermal resistance coefficients, respectively, R high = 0.25 h.m2.K/Kj and R low = 0.5 h.m2.K/Kj) and parametric analysis of ρ = 0.2, 0.55 and 0.8 reflectivity ratio. In every case the Kirchhoff's law retained, so as,

$$\alpha + \rho = 1 \quad (6)$$

It was observed that the difference between the cooling loads of the exposed and pv shaded roof, as percentage, maximized with the decrease of their thermal resistance and increase of reflectivity value. In Figure 2.3a the pv shading effect on cooling loads of the less insulated and the more reflective roofs for the specified period is presented, while in figure 2.3b the zone temperature of the lumped capacitance model and different U factors are simulated with initial value Tz = 20oC. The more insulated buildings present larger attenuation in temperature variations, as expected. The above results are similar to those of Kolokotroni et al. (Kolokotroni M. et al, 2011)

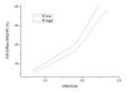

Figure 2.3a: PV shading effect vs thermal resistance R and reflectivity ρ

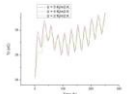

Figure 2.3b: Simulated lumped capacitance zone temperature vs U factors

The roof experimental conditions of 7.5 cm (3'') XPS extruded polystyrene insulation and concrete slab were subsequently selected to study the cooling loads and peak demand
The temperature difference between the bare and PV covered roof surface has a simultaneous impact on the heat flux downwards or upwards the building room conditions. Since the thermal resistance of the ceiling is known, according to the materials properties, the heat flux was modeled as above, taking into account the Fourier uniform heat transfer equation and the steady state heat loss coefficient. The thermal resistance was considered the same for the whole roof with a value R = 0.72 h.m2.K/Kj. In all cases the back edge pv thermal resistance is constant and equal to Rpv = 0.15 h.m2.K/Kj.

The recorded negative differences in values are corresponding to a decrease in cooling loads with the BAPV installation, primary, due to decreased heat flux (heat gain) coming from the roof surface. The peak load demand is also reduced during the on peak solar radiation hours and a cumulative effect occurs during the whole (Figure 2.3c). In a daily basis the reverse heat flux observed at night in both roofs, while at the same time the roof surface temperatures changed order with the exposed roof becoming lower (Figure 2.3d).

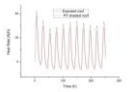

Figure 2.3c: Cooling loads and peak load demand for exposed and PV shaded roof

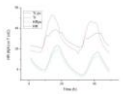

Figure 2.3d: Daily surface temperatures and heat rates comparison

At the same period a comparison made between the cumulative cooling effect and the cumulative cooling degree hours derived by the following formula,

$$CDH = \quad N_i * \quad {}_i \max\{0,\ Ti, air - Tref\ \} \quad (7)$$

where, Ni in hours, Ti,air the hourly average air temperature derived from the meteorological station and Tref a reference temperature, here 26oC (Figure 2.3e).

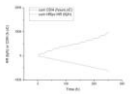

Figure 2.3e: Cumulative Cooling Degree Hours and cumulative PV shading cooling effect

The present study indicates that the roof BAPV leads to passive energy savings for an extended time period in addition to energy production for specific environmental conditions. Therefore, loads variation is highly sensitive to the selection of the environmental parameters for the particular location, PV tilt angle installation and the building structural materials. Thus, it is proposed that a detailed simulation of the building energy loads should be performed before the BAPV installation at a particular building of a specific location in order to optimize their positive shading effects in addition to their energy production.

2 CONCLUSIONS

The temperatures of the experimental study validated and simulated with quite success through TRNSYS engine. Then, the heat fluxes examined for two cases of thermal resistances and three different albedos, concluded that positive cooling effect increases at poor insulated and high reflectivity buildings. The zone temperature is simulated for three different U values and resulted to a better attenuation of the better insulated one. Eventually, the cumulative correlation of cooling effect and cooling degree hours denotes that a better insight is needed all over the year's demand response.

The cooling load study with the results presented above revealed a significant positive cooling effect of the BAPV within the specified period and conditions. The cooling energy demand response of the building reduced as well as the high cooling demand on peak or nearby radiation hours. The additional simultaneous renewable power production is an additional beneficial aspect to consider due to the environmentally cost reduction and the net metering advantages for the owner.

In a daily basis observation the surface temperature's order is reversed at night, with the exposed roof's being the smaller. It seems that at pv shaded surface the long wave radiation is trapped between the roof and the back pv array surface with reduced emissivity, while at the same time the exposed roof higher view factor at night sky leads to a faster cooling, at least at the upper and external layers of the roof.

However, the lumped capacitance method which used to analyse the effect in our model, presented limitations and is a rough estimation of the heat transfer process and the impact of the PV array which occurred. The thermal mass of the roof is unchanged, the effective temperature which depended on the effective conductance is unchanged, too, and the same zone temperature in both cases is used. On the other hand, the sensitivity of the model in different conditions and material properties should be simulated and investigated more and the findings have to exposed in a larger time period and more environmental and other factors.

3 REFERENCES

[1] Santamouris M., Papanikolaou N., Livada I., Koronakis I., Georgakis C., Argiriou A., Assimakopoulos D.N. (2001). On the impact of urban climate on the energy consumption of buildings. *Solar Energy*, 70(3), 201-216.

[2] Giannopoulou K., Livada I., Santamouris M., Saliari M., Assimakopoulos M., Caouris Y.G. (2010). On the characteristics of the summer urban heat island in Athens, Greece. *Sustainable Cities and Society*, 1(1), 16-28.

[3] Vardoulakis E., Karamanis D., Mihalakakou G., Assimakopoulos M.N. (2011). Heat island effect in Western Greece: results, statistical analysis and discussion. In: Kungolos A., Karagiannidis A., Aravossis K., Samaras P., Schramm K.W., editors. *Cemepe 2011: Proceedings of the third International Conference on Environmental Management, Engineering, Planning and Economics*, June 19-24, Skiathos.

[4] Vardoulakis E., Karamanis D., Assimakopoulos M.N, Mihalakakou G. (2011). Solar cooling with aluminium pillared clays. *Solar Energy Materials and Solar Cells*, 95(8), 2363-2370.

[5] Karamanis D., Vardoulakis E. (2012). Application of zeolitic materials prepared from fly ash to water vapor adsorption for solar cooling, 97, 334–339.

[6] Synnefa A., Santamouris M., Livada I., (2006). A study of the thermal performance of reflective coatings for the urban environment. *Solar Energy,* 80(8), 968-981.

[7] Alvarado J.L., Terrell Jr.W., Johnson M.D. (2009). Passive cooling systems for cement-based roofs. *Building and Environment*, 44(9), 1869-1875.

[8] Greek operator of electricity market. (2012). *http://www.lagie.gr/ape-sithya/miniaia-deltia-ape/*, accessed at August 5th.

[9] Strzalka A., Alam N., Duminil E., Coors V., Eicker U. (2012). Large scale integration of photovoltaic in cities. *Applied Energy*, Article in press.

[10] James P.A.B, Jentsch M.F., Bahaj A.S. (2009). Quantifying the added value of BIPV as shading solution in atria. *Solar Energy*, 83(2), 220-231.

[11] Dominguez A., Kleissl J., Luvall J.C. (2011). Effects of solar photovoltaic panels on roof heat transfer. Solar Energy, 85(9), 2244-2255.

[12] Wang Y., Tian W., Ren J., Zhu L., Wang Q. (2006). Influence of a building's intergrated-photovoltaics on heating and cooling loads. *Applied Energy*, 83, 989-1003.

[13] Tian W., Wang Y., Xie Y., Wu D. Zhu L., Ren J. (2009) Effect of building integrated photovoltaics on microclimate of urban canopy layer.

[14] Yang H., Zhu Z., Burnett J., Lu L. (2001). A simulation study on the energy performance of photovoltaic roof , *ASHRAE Transactions*, 107(2), 129-135

[15] Scherba A., Sailor D.J., Rosenstiel T.N., Wamser C.C. (2011). Modeling impacts of roof reflectivity, integrated photovoltaic panels and green roof systems on sensible heat flux into the urban environment. *Building and Environment*; 46, 2542-2551.

[16] TRNSYS, (2010). The Transient Energy System Simulation Tool, *http://www. trnsys.com/about.htm*.

[17] ASHRAE (2013). ASHRAE Handbook – Fundamentals. Atlanta, GA: *American Society of Heating, Refrigerating and Air-Conditioning Engineers*, Inc. (Chapter 26, Heat, Air and Moisture control in buildings assemblies – Material properties).

[18] Kolokotroni M., Gowreesunker B.L., Giridharan R., (2011). Cool roof technology in London An experimental and modeling study, *Energy and Buildings*, Article in press.